Buckling of Amphiphilic Monolayers Induced by Head-Tail Asymmetry

J.-G. Hu, R. Granek

Buckling of Amphiphilic Monolayers Induced by Head-Tail Asymmetry

J.-G. Hu and R. Granek (*)

Department of Materials and Interfaces, Weizmann Institute of Science, Rehovot 76100, Israel

(Received 2 October 1995, received in final form and accepted 27 March 1996)

PACS.82.65.Dp – Thermodynamics of surfaces and interfaces
PACS.68.10.-m – Fluid surfaces and fluid-fluid interfaces
PACS.47.20.Dr – Surface-tension-driven instability

Abstract. — Packing asymmetry between head-group and tail-chain of amphiphiles may induce buckling modulations in monolayers at air-water or oil-water interfaces. We consider three different cases associated with the head-tail asymmetry: (i) spontaneous curvature, (ii) molecular tilt divergence, and (iii) local composition variation in mixed monolayers. For a pure monolayer with non-zero spontaneous curvature, we find that, below some critical surface tension, an hexagonal array of "long-fingers" becomes more stable than the flat surface. This "long-finger" structure is not expected to remain stable against multilayer formation in the case of a Langmuir monolayer, but is relevant for monolayers at the oil-water interface. When the molecular tilt is non-zero, as often is the case in the liquid condensed phase of Langmuir monolayers, the coupling between curvature and tilt can also give rise to a first-order buckling transition. Considering a binary mixture monolayer, we find that it can easily buckle to periodic structures following composition modulations. For the latter case we find two kinds of buckling structures. One involves a very large amplitude, a counterpart of the "long-finger" structure, and is dominated by the average spontaneous curvature. The other structure is of much smaller amplitude, and results from the curvature-composition coupling. Implications for the process of spontaneous emulsification are also briefly discussed.

1. Introduction

Monolayers of amphiphilic interfaces are important to the design of new materials and are challenging systems which allow one to study the transition from 2- to 3-Dimensional (3D) physics and chemistry [1]. Their importance in applications such as coatings, catalysts, and surface tension modifiers requires an understanding of their equilibrium structure and stability, as related to their failure to remain as simple monolayers. There are also related biological issues; for example, understanding the stability of monolayers may also shed some light on key aspects of the behavior of the lungs [2], which involve a Langmuir monolayer covering a few microns thick solution, sitting on top of the living tissue.

A Langmuir monolayer under compression, sitting at the liquid-air surface, can explore the third dimension in several ways. As the surface pressure is increased the monolayer may *buckle* [3–5], namely become weakly corrugated or simply bent, or it may even fully "collapse"

(*) Author for correspondence (e-mail: cpgranek@weizmann.weizmann.ac.il)

by folding over itself to form trilayer or multilayer structures. (The term "collapse" is often referred to as the formation of the 3D bulk phase, while formation of a few layers or possibly buckling are sometimes referred to as "partial collapse".) It is also hypothetically possible that the buckling will be followed immediately by the formation of multilayers, in which case the buckling state will not be observed. For a monolayer at the oil-water interface, on the other hand, it is much more plausible that the monolayer to multilayer transition will not appear at all, because of the absence of real energy gain in the formation of multilayers. In this case, however, a large amplitude buckling is not likely to stay stable for a long time, and may lead to spontaneous emulsification [6].

From the experimental viewpoint, monolayers at the air-water surface often "collapse" to form multilayers [2, 7–11], while a buckling transition has been reported so far only in two experiments [4, 5]. In the study of Saint-Jalmes *et al.* [5] a second order buckling transition of a solidified monolayer (with a non-zero tilt angle) has been directly observed by shadowgraphy and more quantitatively by light scattering experiment. The work of Bourdieu *et al.* [4] deals with a polymerized monolayer. In this paper, instead, we would like to focus on Langmuir monolayers which are still in their liquid or liquid-crystalline-like phases, *i.e.*, either liquid expand or liquid condensed phases. As suggested by several authors [7, 10] (on a purely qualitative basis), it is possible that a buckling state is often the transition state that allows fast nucleation of multilayers.

Moreover, pressure-area isotherms of quite different systems, *e.g.*, fatty acid monolayers [10,12,13], often show a plateau at high applied pressures $\Pi_{ex} \simeq 65-70$ dyne/cm corresponding to areas per molecule smaller than the close packing area. It is sometimes hard to interpret this plateau as either a monolayer to multilayer transition, or as the point of transition from insoluble to soluble monolayer. For example, in a stearic acid monolayer a clear plateau in the isotherm is observed [10] when the area per molecule is decreased below 20 Å^2 (down to $\sim$ 1 Å^2) and for pH > 6 (with $\Pi_{ex} \simeq 65$ dyne/cm). As the pH is lowered, a dip appears in this plateau which widens out to finally make a lower new plateau, with only an overshoot left from the initial plateau. This new (lower) plateau has been interpreted as a monolayer to trilayer coexistence [10], an assumption which has been partially confirmed by atomic force [13], and Brewster angle [12] microscopies. (The lower pH presumably facilitates the formation of hydrogen bonds.) A monolayer to trilayer transition has also been observed in several other systems [11, 14, 15]. What is left unclear, then, is the (higher) plateau in this system observed at pH$>$ 6. It is quite possible that this plateau corresponds to a first order buckling transition, although this hypothesis is yet to be confirmed by direct measurements.

From the theoretical viewpoint, a buckling instability has been predicted by Milner *et al.* [3] for negative surface tensions. This however is not entirely relevant for monolayers at the air-water surface as these tend to form multilayers already at positive tensions. Another very interesting, but not yet well founded, suggestion, has been that of a dipolar interaction effect [5]. Other approaches focused on composition modulation effects in binary systems [16–18], and on persistence length effects [19]. Closely related questions in lamellar [20,21] and vesicular [22,23] bilayer systems have been also addressed. One important quantity that was not fully accounted for in these previous (theoretical) studies of monolayers is the *spontaneous curvature* of the film. The spontaneous curvature results from differences in preferred areas of the heads and tails and thus breaks the symmetry between up and down (air and water, or oil and water). It can possibly make the buckling transition be first order and happen at *positive tensions*, as further discussed in Section 2. (The spontaneous curvature was included in a few theoretical studies of vesicle shapes [22], which could be related to the present study in the limit of infinite vesicle size.)

Our description thus far has been concerned with the buckling of a pure surfactant monolayer. In many practical and biological applications, however, monolayers are composed of a few components. One example is the lung surfactant, which is a mixture of lipids, fatty acids and proteins and form monolayers at the alveolus air-water interface [2], thereby reducing the surface tension to almost zero. Ink varnish monolayer is also a mixture of polymeric amphiphiles which can even bear a slightly higher pressure than air-water surface tension [24]. These studies show that multicomponent monolayers can have very different behaviour from the pure systems. In this work we consider (in Sect. 3) a binary mixture and characterize each component in the mixture by its own spontaneous curvature, leading to a coupling between composition and curvature. As first pointed out by Leibler and Andelman [16], and later by Wang [17] and by Andelman *et al.* [22, 23], this coupling may lead to a modulation of composition and curvature. Our objective here is to include into these previous studies the non-linear symmetry-breaking effect generated by a *net average spontaneous curvature* (*i.e.*, the one which results from random mixing). This leads again to a first order buckling transition upon increasing the surface pressure (and so to a plateau in the isotherm), as opposed to the mostly second order nature of the transition occurring when the non-linear bending terms are neglected. Unlike in the case of a pure monolayer, we find in Section 3 that for strong coupling, which occurs when the two spontaneous curvatures are similar in magnitude but have opposite signs, the amplitude of the buckling state is now relatively small.

A similar degree of freedom, which could be relevant for both single- and multi- component systems at the liquid-air surface (but usually not for oil-water interfaces), is the tilt of the surfactant molecule with respect to the surface normal. This usually occurs in monolayers their liquid condensed phase [25]. If the tilt is coupled to the curvature, it can induce a buckling transition which will also break the symmetry between up and down, in a similar way to the spontaneous curvature. A similar mechanism has been suggested by Mackintosh, Lubensky and Chen [21] to explain the appearance of the ripple phase in phospholipid bilayers. This possible coupling will be therefore studied separately in Section 4.

The study of the buckling transition may also help to understand the process of spontaneous emulsification. It has been recently suggested that large amplitude buckling of an oil-water interface may lead to the formation of small "microemulsion" droplets at the interface [6]. In the latter study, which addressed mainly the dynamics of the process, the mechanism that has been suggested involves a slightly negative surface tension, similar to the study of buckling by Milner *et al.* [3]. In addition, the effect of spontaneous curvature was not truly accounted for, and so it was not possible to determine whether it is oil in water, or water in oil, droplets, which are spontaneously formed at the oil-water interface. A transition to a non-symmetric buckling state will clearly be a route to this important selection.

In this paper we primarily study the effect of the up-down asymmetry on the buckling of a monolayer. This asymmetry is modeled in two ways. In the first case (Sect. 2) we use the Gibbs free-energy which includes the Helfrich bending Hamiltonian with non-zero spontaneous curvature. This is generalized in Section 3 to account for a non-zero *average* spontaneous curvature in binary mixtures. In the second case (Sect. 4) we couple the curvature to a tilt order parameter and use a free-energy for the tilt which is non-symmetric with respect to reflection. Free-energies are minimized both analytically and numerically using variation ansatzs for the buckling state that incorporate the asymmetry between the two sides. We note that although our approach does not distinguish between monolayers at air-water and at oil-water interfaces, our results do have different implications on them. This is discussed in Sections 5 and 6.

2. Bending Free-Energy – General Approach

Our starting point is the construction of the Gibbs free-energy for a monolayer held at a fixed external pressure Π_{ex}. The monolayer is allowed to buckle in the third dimension. In this case the measured trough area, which we call the projected area A_o, is smaller than the real monolayer area A. The Gibbs free-energy is expressed as [3]

$$G = \gamma_o(A - A_o) + Af_o(c_s) + F_\kappa + \Pi_{ex}A_o \tag{1}$$

The first term accounts for the fact that, in a hypothetical change from a flat state to a buckled state of the same area A, a pure air-water surface of area $A - A_o$ – and bare surface tension γ_o – is exposed. The second term is the part of Helmholtz free-energy of the monolayer which does not depend on curvature; $f_o(c_s)$ is the free-energy density and $c_s = N/A$ is the concentration of amphiphiles on the actual (possibly buckled) surface. F_κ is the curvature dependent part of the free-energy, and the last term, $\Pi_{ex}A_o$, is the usual Legendre transform,"PV", term, expressing the mechanical work done on the system.

Different buckled states of the same area A may have different projected areas A_o. The buckled state is uniquely specified by the "height" deviation function $h(\mathbf{x})$ (where $\mathbf{x}$ is a 2D vector on the reference flat surface), assuming, for simplicity, that no overhangs are allowed, *i.e.*, $h(\mathbf{x})$ is a single valued function. Given $h(\mathbf{x})$, the relation between A and A_o is given by

$$A = \int_{A_o} \mathrm{d}^2x\sqrt{g} \tag{2}$$

with

$$g = 1 + (\nabla h)^2 \tag{3}$$

The equilibrium state can be found by minimizing G over A, A_o, and all possible buckling states $\{h(\mathbf{x})\}$, subject to the constraint (2). This constraint is incorporated using the Lagrange multipliers method, in which we introduce the surface tension σ as the Lagrange multiplier. We thus minimize

$$G_\sigma = G - \sigma\left(A - \int_{A_o} \mathrm{d}^2x\sqrt{g}\right) \tag{4}$$

with no constraints. For clarity, G_σ is rewritten as

$$G_\sigma = [\gamma_o + f_o(c_s) - \sigma]\,A - (\gamma_o - \Pi_{ex})\,A_o + F_h \tag{5}$$

with

$$F_h = \sigma\int_{A_o} \mathrm{d}^2x\sqrt{g} + F_\kappa \equiv F_\sigma + F_\kappa \tag{6}$$

Note that F_h has the more familiar free-energy form which incorporates both surface tension and bending energy.

Let us now specify the bending free-energy F_κ. For small curvatures it is given by the Helfrich Hamiltonian [26]

$$F_\kappa = \frac{1}{2}\kappa\int_{A_o} \mathrm{d}^2x\sqrt{g}\,(H^2 - 2HC_o) \tag{7}$$

Here C_o is the spontaneous curvature, κ is the bending modulus, and H is the mean curvature,

$$H = \frac{1}{R_1} + \frac{1}{R_2} \tag{8}$$

where R_1 and R_2 are the local radii of curvature. The curvature is taken positive when the surface is concave. (The Gaussian curvature $1/(R_1R_2)$ was omitted in equation (7) since we do not consider here topological transformations of the surface.) H is related to the surface normal $\hat{\mathbf{N}}$ by $H = \nabla \cdot \hat{\mathbf{N}}$ leading to

$$H = -\nabla \cdot \frac{\nabla h}{\sqrt{g}} \tag{9}$$

(Gradients here are 2D and are defined on the reference planar surface.) Note that in F_κ we choose to keep only curvatures dependent terms; other constant terms are absorbed into $f_o(c_s)$. We neglect any possible dependence of κ and C_o on the monolayer concentration c_s.

We shall consider (for simplicity) only periodic buckling structures, denoting by a_λ the area of a periodic (Wigner-Seitz) cell. Integrals are then transformed according to

$$\int_{A_o} \mathrm{d}^2x \,.. = \frac{A_o}{a_\lambda} \int_{a_\lambda} \mathrm{d}^2x \,.. \tag{10}$$

so that the free-energy density $f_h = F_h/A_o$ is independent of A_o.

We now turn to the minimization of G_σ over A, A_o, and all possible buckling states $\{h(x,y)\}$. Minimizing over A_o and A (recalling that $c_s = N/A$) we obtain

$$\Pi_{ex} = \gamma_o - f_h \tag{11}$$

$$\sigma = \gamma_o - \Pi(A) \tag{12}$$

with the *internal* monolayer surface pressure $\Pi(A)$ as usual given by

$$\Pi(A) = -\partial(Af_o(c_s))/\partial A \tag{13}$$

Inserting σ from equation (12) into equation (6) and using (11) yields a *general* relation between the *internal* pressure and the *external* pressure in the form

$$\Pi_{ex} = \gamma_o - \frac{(\gamma_o - \Pi(A))}{a_\lambda} \int_{a_\lambda} \mathrm{d}^2x\sqrt{g} - \frac{\kappa}{2a_\lambda} \int_{a_\lambda} \mathrm{d}^2x\sqrt{g}\,(H^2 - 2HC_o) \tag{14}$$

Only when $f_h = \gamma_o - \Pi(A)$, as for, *e.g.*, a flat surface, do we obtain $\Pi_{ex} = \Pi(A)$. When $\gamma_o - \Pi_{ex} = f_h < \gamma_o - \Pi(A)$ we have $\Pi_{ex} > \Pi(A)$. This may be understood by noting that in a given buckled state which is away from the transition, both the bending forces and the internal monolayer pressure work to balance the external pressure. To find Π_{ex} for such a state one needs to know of course the monolayer equation of state $\Pi(A)$; this is not our main scope here.

Suppose that the monolayer goes through a first order buckling transition, as shown later. At the transition, on both flat and buckled states, $f_h = \gamma_o - \Pi(A)$ and so $\Pi(A)|_{\text{buckled}} = \Pi(A)|_{\text{flat}} = \Pi_{ex}$. Accordingly the monolayer area A *does not change* through the transition. This important conclusion allows us to deal with the transition without having to specify the equation of state $\Pi(A)$. Of course, we cannot predict in this way the "critical" area A_o $(= A)$ of the flat state at the transition, but, on the other hand, we can calculate the ratio A_o/A (for the buckled state), which determines the relative width $1 - A_o/A$ of the coexistence plateau in the pressure-area isotherm. (Recall that for the flat state $A_o = A$ while for the buckled state $A_o < A$.)

For the buckled state at the transition, we are thus left with the minimization of G_σ over the manifold of states $\{h(\mathbf{x})\}$. This involves only the free-energy F_h defined in equation (6) with

$\sigma = \gamma_o - \Pi_{ex}$. The same expression is involved if we explicitly use the fact that A does not change through the transition. With this assumption the Gibbs free-energy difference between buckled and flat states (at transition) becomes

$$\Delta G = G^{(b)} - G^{(f)} = (\gamma_o - \Pi_{ex})(A - A_o) + F_\kappa \tag{15}$$

in which ΔG differs from F_h only by an additive constant. In fact, equation (15) could have been our starting point, but we have chosen to start with the more general procedure since it also allows in principle calculations away from the transition and at metastability.

Led again by the fact that ΔG should exhibit a first order transition as Π_{ex} increases, we can envisage several local minima corresponding to different buckling states ($h \neq$ const.). When ΔG of the global minimum vanishes, a transition from flat to the corresponding state occurs. Alternatively, each buckling state can be associated with a fictitious critical pressure $\Pi_c \equiv \Pi_{ex}^{(crit)}$ (for which $\Delta G = 0$), so that the lowest critical pressure determines the real transition. Putting $\Delta G = 0$ in equation (15) and solving for Π_c we obtain

$$\Pi_c = \gamma_o + \frac{F_\kappa}{A - A_o} \tag{16}$$

or, more explicitly,

$$\Pi_c = \gamma_o + \frac{\frac{1}{2}\kappa \int_{a_\lambda} d^2x \sqrt{g}\,(H^2 - 2HC_o)}{\int_{a_\lambda} d^2x\,(\sqrt{g} - 1)} \tag{17}$$

(Of course, putting $\Pi(A) = \Pi_{ex}$ in Eq. (14) and solving for Π_{ex} will lead to the same result.)

Minimizing Π_c over $\{h(x,y)\}$ requires however solution of the Euler-Lagrange equations, which are highly non-linear partial differential equations for this case. We therefore use a variation approach using trial functions. The trial function which will give the lowest critical pressure is the closest one to the true buckling shape. Obviously, the trial function should not be symmetric with respect to the two sides of the monolayer if the effect of spontaneous curvature is to be accounted for correctly. Let us first distinguish between 1D and 2D buckling shapes.

For 1D (stripe) buckling in which the shape function is mathematically analytical, we can use in equation (7) (say) $R_2 = \infty$ and $R_1 = R(\zeta)$, where ζ is a curvilinear coordinate. The term involving C_o simply becomes

$$L\kappa C_o \int \frac{d\zeta}{R(\zeta)} = L\kappa C_o \int d\theta = L\kappa C_o(\Theta_R - \Theta_L) \tag{18}$$

where θ is the angle describing the direction of the tangent to the curve, $\Theta_{R,L}$ are the corresponding angles at the boundaries, and L is the system linear size. The spontaneous curvature has thus *no effect* on the "bulk" surface shape, although some effects could be present near the boundaries.

We therefore turn to examine non-symmetric 2D buckling shapes. We choose to use triangular (hexagonal) periodic functions, for which the asymmetry occurs already in the first harmonic (see Fig. 1). Let us begin by considering first the regime $\nabla h \ll 1$. We expand both the numerator and denominator of equation (17) up through the six-th order in h, which is required for stability. We then use only the first harmonic of hexagonal periodicity (Fig. 1)

$$h(\mathbf{x}) = h_o \left[\cos(qx) + \cos\left(q\frac{-x + \sqrt{3}y}{2}\right) + \cos\left(q\frac{x + \sqrt{3}y}{2}\right)\right] \tag{19}$$

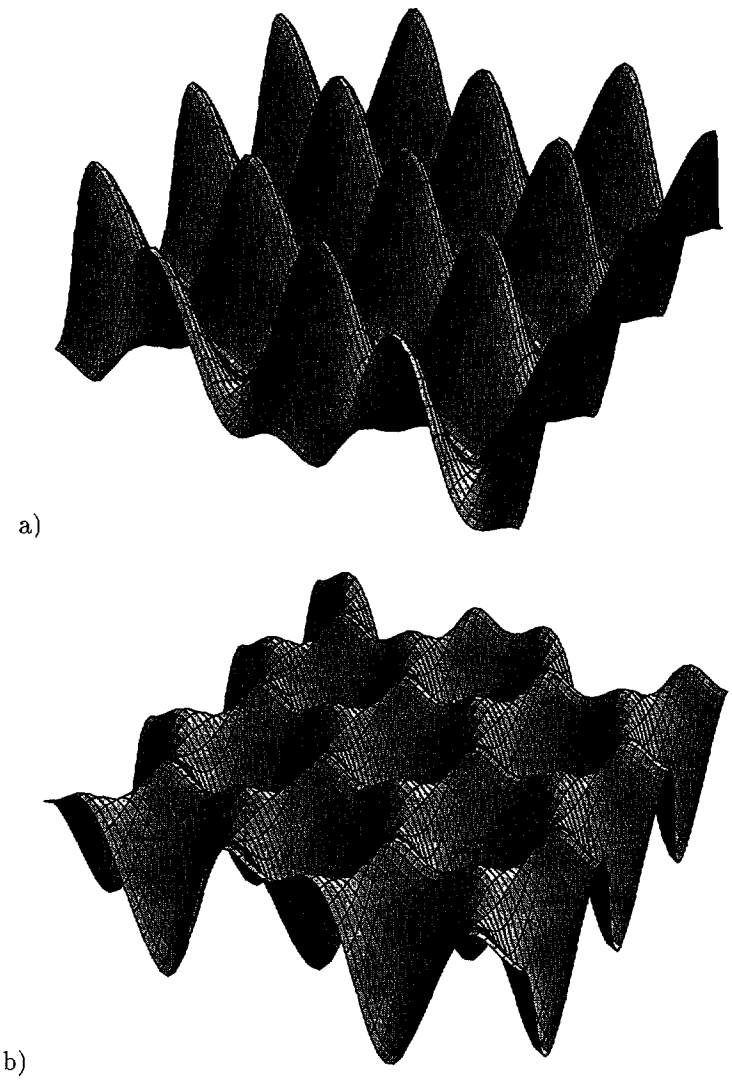

Fig. 1. — The first harmonic of hexagonal buckling, equation (19) ($h_o = q$): (a) is for $h_o > 0$; (b) is for $h_o < 0$ and is also the view from bottom to top of (a). ((b) is referred to in the text as inverse-hexagonal.)

Performing the integrals in equation (17) and simplifying the result, we obtain

$$\Pi_c = \gamma_o + \kappa q^2 \frac{16 + 8C_o h_o - 26q^2 h_o^2 - 12C_o q^2 h_o^3 + 65q^4 h_o^4}{16 - 9q^2 h_o^2 + (91/8)q^4 h_o^4} \tag{20}$$

We now have to minimize Π_c over both the amplitude h_o and wavenumber q. From dimensional considerations we may expect that the values corresponding to the minimal shape will scale with C_o according to $q_c \sim C_o$ and $h_{oc} \sim C_o^{-1}$. Indeed, putting $q = \alpha C_o$ and $h_o = \beta C_o^{-1}$ (where α and β are numerical constants) we obtain $\Pi_c = \gamma_o + \nu\kappa C_o^2$ where ν is a numerical constant depending on α and β. Minimizing Π_c thus amounts to minimizing ν over α and β, and we find

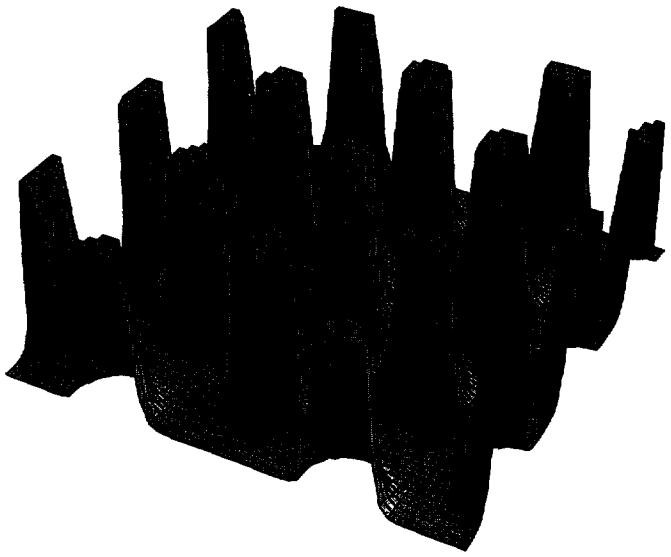

Fig. 2. — Illustration of the long finger buckling shape obtained from equation (21). The vertical scale was reduced (*i.e.*, the actual values of W_{oc}, u_{oc} and q_c were not used) and the top part of the figure was chopped for the purpose of representation. Compare to Figure 1.

(numerically) $q_c = 0.05C_o$, $h_{oc} = 29.8C_o^{-1}$ and $\Pi_c = \gamma_o - 0.0133\kappa C_o^2$. The ratio of projected area A_o to real area A in the buckled state (at the transition) is $A_o/A = 0.156$. Recall that since A does not change through the transition, this ratio determines the relative width of the plateau in the pressure-area isotherm. Note that the sign of the spontaneous curvature C_o determines if it is hexagonal ($h_o > 0$) or inverse-hexagonal ($h_o < 0$) buckling shape which is obtained (see Fig. 1).

As expected we have found $\gamma_o - \Pi_c \sim \kappa C_o^2$, however, the numerical prefactor ν obtained is much smaller than unity. We attribute this to the insufficient adequacy of our trial function — the first harmonic of the hexagonal symmetry — which only slightly breaks the up-down symmetry. (The average curvature for the above minimal shape is $\langle H \rangle = 0.0087C_o$.) We also note that our minimal buckling shape obeys $q_c h_{oc} \simeq 1.5$, signifying a breakdown of our expansion, which assumes $qh_o \ll 1$. In view of these, we now seek to go beyond the expansion and beyond the first harmonic of hexagonal symmetry. We shall therefore use the following ansatz

$$h(\mathbf{x}) = W_o \exp\left\{u_o\left[\cos(qx) + \cos\left(q\frac{-x+\sqrt{3}y}{2}\right) + \cos\left(q\frac{x+\sqrt{3}y}{2}\right)\right]\right\} \qquad (21)$$

which is able to more appreciably break the up-down symmetry and mixes high order harmonics. Substituting this function in equation (17) and performing *exact* numerical integration, the absolute minimum is found to be at $q_c = 0.355C_o$, $W_{oc} = 2.5C_o^{-1}$ and $u_{oc} = 3.55$, leading to $\Pi_c = \gamma_o - 0.314\kappa C_o^2$ and $A_o/A = 4 \times 10^{-6}$ This result thus corresponds to an hexagonal array of *extremely long "fingers"* (see Fig. 2) whose length is about $l_c = 8.7 \times 10^4 C_o^{-1}$, which can be macroscopic. As expected, the numerical prefactor $\nu = 0.314$ appearing in the result for Π_c is now of order unity, and so Π_c is significantly smaller than the one obtained using the expansion in single harmonics.

We may understand the high stability of these long fingers (subject, of course, to our trial function) using the following consideration. Consider first the energy associated with end caps. A positive (concave) quasi-hemispherical cap can indeed be adjusted to the spontaneous curvature and give a negligible bending energy contribution, however, the penalty resulting from an identical negative (convex) cap will be too large to be compensated for by this adjustment. Thus the asymmetry between maxima and minima in the hexagonal array can only slightly lower the free-energy density. The energy is much more significantly reduced in the case of long fingers because the core of a finger approaches a *cylindrical* shape, whose *radius is adjusted to the spontaneous radius of curvature.* Using this idea let us now estimate Π_c for the case of perfect, cylindrically shaped, fingers of circular radius $R = C_o^{-1}$ Denoting their length as l we obtain from equation (16)

$$\Pi_c = \gamma_o + \frac{E_{caps} - \pi\kappa l C_o}{A_{caps} + 2\pi l/C_o} \tag{22}$$

with E_{caps} and A_{caps} denoting the energy and area associated with end caps. For $l \to \infty$ this becomes

$$\Pi_c = \gamma_o - \frac{1}{2}\kappa C_o^2 \,, \tag{23}$$

showing that the numerical prefactor (ν) should indeed be of order unity, but cannot be in fact larger than 1/2. Note that the resulting critical surface tension, $\sigma_c = \kappa C_o^2/2$, is just the tension of a flat soluble monolayer under conditions of complete saturation.

To see if this exotic shape can be reached by a thermal fluctuation at the thermodynamic phase transition we have to look at the energy barrier. Taking $\kappa \simeq 30 k_B T$ and $C_o^{-1} = 40$ Å, the lowest barrier we are able to find (numerically) corresponds to $\sim 10^3 k_B T$ per buckling period. It is therefore essentially impossible that the buckling state will be reached at the equilibrium transition point without an external excitation. (Of course, the high of this barrier, at the transition, is proportional to κ, so that for $\kappa \sim k_B T$ it is $\sim 10^2 k_B T$, which is still rather high.) As the pressure is further increased and passes through γ_o the barrier lowers and vanishes at the spinodal point for the transition. This occurs when the flat surface becomes a local maximum rather than a local minimum on the free-energy surface in the (F, q, h_o) configuration space. We thus look for the second differential d^2G and calculate it for a flat surface ($h_o = 0$, $A = A_o$) and for an arbitrarily chosen q. We find

$$d^2G|_{h_o=0} = -\frac{\partial \Pi(A)}{\partial A}(dA)^2 + \frac{3}{2}Aq^2\left[\gamma_o + \kappa q^2 - \Pi(A)\right](dh_o)^2 \tag{24}$$

Only the second term in this expression can become negative, and so the limit of local stability of the flat surface against buckling at wavenumber q is given by $\Pi_{ex} = \gamma_o + \kappa q^2$. The smallest Π_{ex} is obtained for the smallest possible wavenumber $q = \pi/L$ (with L, the system linear size) and the spinodal for the flat monolayer is thus

$$\Pi_{ex} = \gamma_o + \pi^2 \frac{\kappa}{L^2} \simeq \gamma_o \tag{25}$$

It is not surprising that this is just the threshold obtained by Milner *et al.* [3] for a (second order) buckling transition in the absence of spontaneous curvature. It is also of interest to find the spinodal of the buckled state. This occurs when the buckled state local minimum combines with the barrier and becomes an inflection point. We thus obtain numerically $\Pi_{ex} \simeq \Pi_c - 0.3\kappa C_o^2$ for the spinodal pressure. We see that this still corresponds to a relatively high pressure, $\gamma_o - \Pi_{ex} \sim \kappa C_o^2$. Pressure-area isotherms often show similar hysteresis under compression and expansion, although the hysteresis we obtained here is indeed a very small one.

We have been concerned so far solely with the absolute minimum of the free-energy. As discussed above, the long fingers solution is not easily accessible because of the too high energy barrier involved. It is therefore of interest to search also for local minima which may have a smaller energy barrier. The only other minimum which we were able to find is at the low cutoff value $q = \pi/L$. Adding gravity to the problem shifts this low cutoff value to much shorter wavelengths [3], however the corresponding critical pressure is (slightly) larger than γ_o. It thus appears that, within our assumption of having no overhangs, the long fingers solution is the only buckling shape to be considered for the bending free-energy (at positive surface tensions) [27]. Of course, it is possible that by forming "beads" these fingers may further lower their free-energy. This will be briefly discussed in Section 5.1.

3. Mixed Surfactant Monolayers

When a monolayer is composed of two components, the local composition may vary from one place to the other depending on the local curvature. Since each surfactant, when forming a single component monolayer, can be characterized by its own spontaneous curvature and bending modulus, in the mixture these quantities will vary from one place to the other, leading to a coupling between curvature and composition. These effects have been previously studied by a few authors, in which a second order buckling transition has been found upon lowering the surface tension [16,17,22]. However, these studies did not take into account the non-linear (high order in h) effects introduced by the spontaneous curvature, as described in Section 2. Wang [17] studied this (second order) type of transition for a monolayer without surface tension, which corresponds to a surfactant-saturated interface. Leibler and Andelman [16] considered a non-zero surface tension, bending free-energy, composition free-energy taken to high order, and composition-curvature coupling. This yielded first order coexistence between flat and (hexagonally) buckled states and between different buckling states upon varying the *composition*, provided that the surface tension is below a given critical value. When the surface tension is varied at a *given* composition [16], they obtain a buckling transition which appears second order (since $q_c = 0$ at the transition). As shown below, a non zero average spontaneous curvature makes this transition always be *first order* and so it can be observed as a plateau isotherm.

For simplicity, we shall consider here only composition variation of the spontaneous curvature, the variation in the local bending modulus being neglected. In addition, we assume that the spontaneous curvature is a linear function of the composition. Namely, given the mole fraction ϕ of (say) component 1, and the two spontaneous curvatures $C_o^{(1)}$ and $C_o^{(2)}$, the resulting spontaneous curvature is

$$C_o = C_o^{(1)}\phi + C_o^{(2)}(1-\phi) \tag{26}$$

Introducing the local composition variation $\Psi(\mathbf{x})$ as $\phi(\mathbf{x}) = \phi_o + \Psi/2$, where ϕ_o is the average of ϕ (and is independent of position), we may write

$$C_o = \bar{C}_o + t\Psi \tag{27}$$

where

$$\bar{C}_o = C_o^{(1)}\phi_o + C_o^{(2)}(1-\phi_o) \tag{28}$$

$$t = \left(C_o^{(1)} - C_o^{(2)}\right)/2 \tag{29}$$

Ψ is thus a scalar order parameter describing the local composition variation from homogeneous mixing ($\Psi = 0$) of the two species. It is bounded according to $-2\phi_o \leq \Psi \leq 2(1-\phi_o)$, where

the lower and upper bounds correspond to the single component case. Equation (27), when inserted into the bending free-energy equation (7), leads to a sum of a bare bending-energy term $F_{\kappa o}$ (in which $\bar{C}_o$ replaces C_o) and a coupling term

$$F_c = -\kappa t \int_{A_o} d^2x\sqrt{g}H\Psi \tag{30}$$

We now need only to specify the free-energy of mixing. To low order in Ψ it may be written as

$$F_\Psi = \int_{A_o} d^2x\sqrt{g}\left(\frac{a_2}{2}\Psi^2 + \frac{b}{2}\left((\nabla\Psi)^2 - (\nabla\Psi\cdot\nabla h)^2/g\right) + \frac{1}{3!}a_3\Psi^3 + \frac{1}{4!}a_4\Psi^4\right) \tag{31}$$

The terms multiplying b are the explicit expression [17] of the square gradient term on a curved surface $(\nabla_s\Psi(s))^2$ in projected base coordinates $(\mathbf{x})$ (and so lead to another, higher order, coupling between Ψ and h). We exclude the possibility that there is an inplane phase transition within a flat monolayer, so that a_2 and b are positive; a_3 can be positive or negative depending on the composition, but a_4 is positive for stability. (a_2 is taken to include the contribution κt^2 resulting from the bending part.) These coefficients can be suitably estimated using the mean-field approximation to the lattice-gas model [28], but we prefer not to invoke this model explicitly. If the composition is nearly symmetrical, $\phi_o \simeq 1/2$, the coefficient a_3 is small [16, 28–30] (assuming that only two body interactions) and so it is sufficient to take only the quadratic terms in order to obtain qualitatively correct results. For non-symmetric compositions, the higher order terms can stabilize the hexagonal phase over the stripe phase [16] and so will be included.

The total free-energy associated with the order parameters h and Ψ, and which is analogous to equation (6), is the sum of the four contributions

$$F_{h\Psi} = F_\sigma + F_{\kappa o} + F_\Psi + F_c \ . \tag{32}$$

We may now repeat the procedure described in Section 2, for the present case. The only difference is that $F_{h\Psi}$, which replaces F_h of Section 2, has to be minimized over both h and Ψ. Thus we find again $\sigma = \gamma_o - \Pi_{ex}$ at the transition. The two states (buckled and flat) have again the same area A. Equating $F_{h\Psi}$ to zero and solving for Π_c we find

$$\Pi_c = \gamma_o + \frac{F_{\kappa o} + F_\Psi + F_c}{A - A_o} \tag{33}$$

Unlike in the case of a pure monolayer with non-zero spontaneous curvature, for a one dimensional buckling, the coupling F_c – resulting from the spatially varying part of the spontaneous curvature – is not simply a constant. We therefore compare the stability of the two symmetries, stripe and hexagonal. The buckling shape h and the composition order parameter Ψ are assumed to have the same phase (based on the result of the linear theory [16, 17], discussed below). For the hexagonal symmetry, $h(\mathbf{x})$ is taken to follow equation (19) and similarly Ψ follows

$$\Psi(\mathbf{x}) = \Psi_o\left[\cos(qx) + \cos\left(q\frac{-x+\sqrt{3}y}{2}\right) + \cos\left(q\frac{x+\sqrt{3}y}{2}\right)\right] \tag{34}$$

For the stripe symmetry we use

$$h(\mathbf{x}) = h_o\cos(qx) \tag{35}$$

and

$$\Psi(\mathbf{x}) = \Psi_o\cos(qx) \tag{36}$$

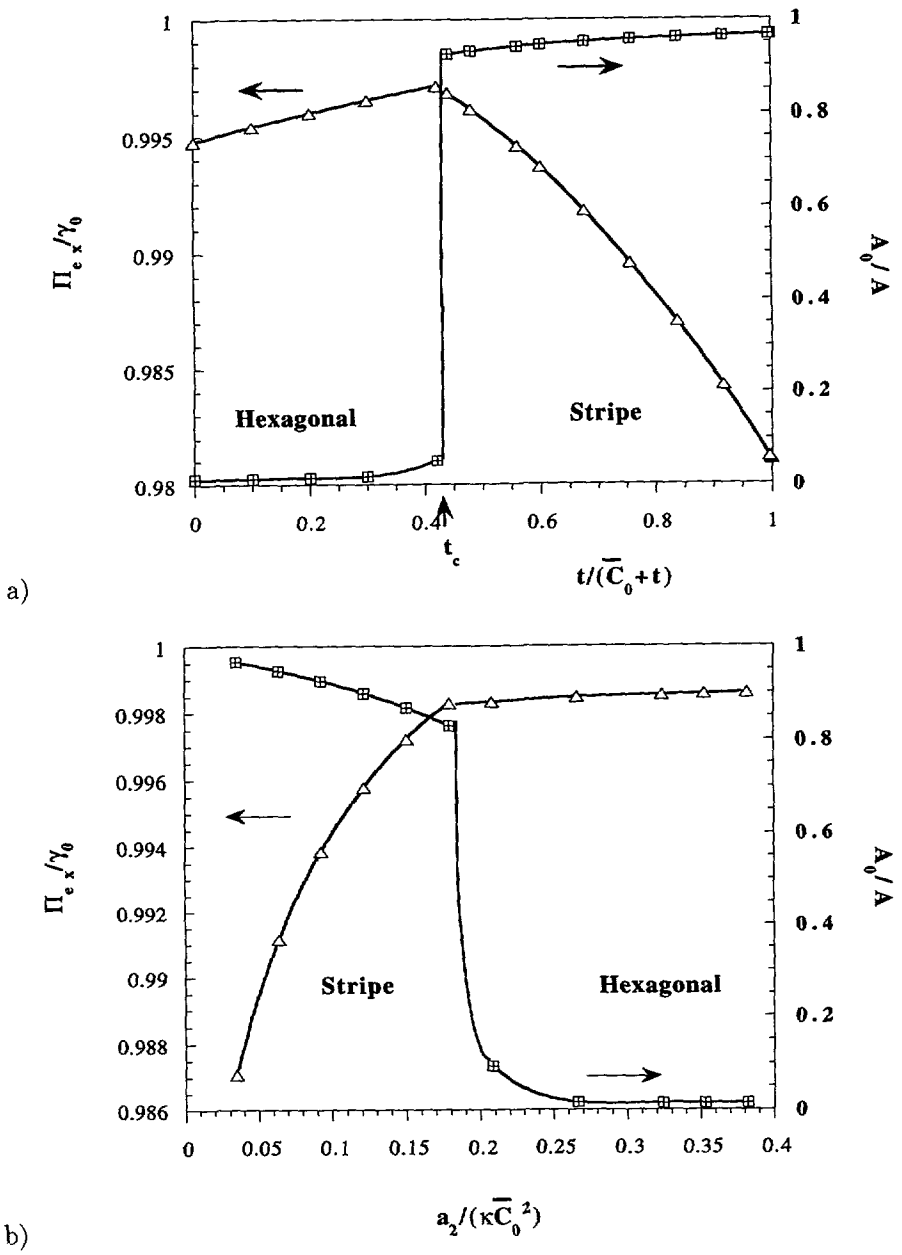

Fig. 3. — Dependence of the external pressure Π_{ex} and the ratio A_o/A of projected area A_o to real area A, on the following three parameters: (a) coupling constant t, (b) coefficient a_2, and (c) coefficient b. The results were obtained by minimizing numerically equation (33) using the trial functions equations (19) and (34) for the hexagonal symmetry and equations (35), (36) for the stripe symmetry. By changing each of the above three parameters, we can see a crossover (denoted by t_c in (a)) from small amplitude buckling of stripe symmetry to large amplitude buckling of hexagonal symmetry. The symbols are numerical data points, the lines are numerical fits to the data, performed separately for the two regimes. (The vertical lines are guides to the eye.) We used $\gamma_o = 71.4$ dyne/cm and $\kappa = 30k_BT$ for all figures. In (a), $a_2 = 2.4 \times 10^{-5} k_BT/\text{Å}^2$, $b = 5\kappa = 150k_BT$. In (b), $t^{-1} = 77$ Å, $b = 30k_BT$ and $\bar{C}_0^{-1} = 83$ Å. In (c), $a_2 = 2.4 \times 10^{-5} k_BT/\text{Å}^2$, $t^{-1} = \bar{C}_0^{-1} = 80$ Å.

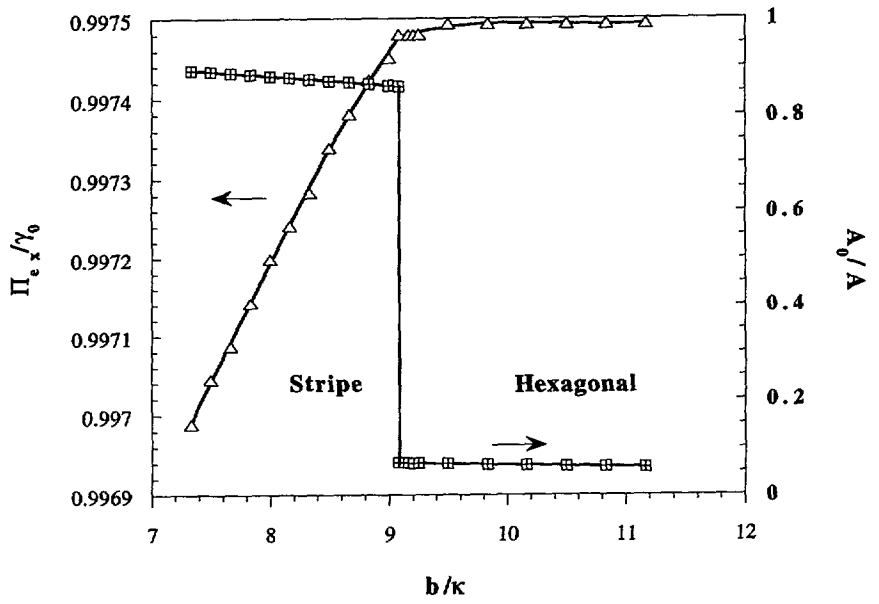

Fig. 3. — *(Continued)*

The resulting Π_c is minimized numerically with respect to h_o, Ψ_o and q, for various coefficients.

Consider first the symmetric (or nearly symmetric) composition case $\phi_o = 1/2$, for which we set [16, 28] $a_3 = a_4 = 0$. (a_4 is set to zero for simplicity.) Our results for this case are summarized in Figure 3. Fixing two of the remaining parameters (a_2, b and t), we always have a crossover from a regime of *stripe* type buckling of *small amplitude* (and $A_o/A \simeq 1$) to a regime of *hexagonal* and *large amplitude* buckling ($A_o/A \ll 1$), reminiscent of the long fingers solution obtained in Section 2. Varying the coupling constant t, we can see from Figure 3a that for large t the stripe (and small amplitude) buckling is preferred while for small t the hexagonal (and large amplitude) buckling is more favorable. There is a critical value of t, $t_c \simeq \bar{C}_0$, that separates the two regimes. In Figures 3b, 3c we can observe similar crossovers when changing either a_2 or b respectively. Note that although Π_c is (of course) continuous when crossing from one regime to the other, the plateau relative width $(1 - A_o/A)$ changes sharply. For typical range of parameters ($\bar{C}_0^{-1} = 80$ Å, $\kappa = 30 k_B T$, $a_2 \sim 10^{-2} - 10^{-6} k_B T/\text{Å}^2$ and $b \sim 0.1 - 10\kappa$), we usually get the wavelength of the buckling state $\lambda_c \sim 1$ μm (for both small and large amplitude bucklings). The amplitude of the small buckling state is about 100 Å, and that of the large buckling state is greater than 1 μm.

When the composition is non-symmetric, namely when a_3 is either positive or negative, the situation is more complicated. To illustrate this we compare here two *different* systems (involving different types of surfactants), both chosen to have the same $\bar{C}_o$, but inversely symmetric composition $\phi_o \to 1 - \phi_o$. (ϕ_o always refers to the mole fraction of surfactant whose spontaneous curvature $C_o^{(1)}$ is the largest of the two.) For large $|a_3|$ (say, for $\phi_o = 1/8$, $7/8$) we find again a crossover bewteen two types of buckling states when the coupling strength t is varied, with the critical value $t_c \gg \bar{C}_o$ for this case (*e.g.*, $t_c \sim 10\bar{C}_o$ for $\phi_o = 1/8$, based on our lattice-gas estimates [28]). For the regime $t > t_c$ (*i.e.*, $t \gg \bar{C}_o$) we find, instead of the stripe buckling, a *small amplitude* buckling of either *hexagonal* (a_3 positive, $\phi_o > 1/2$) or *inverse-hexagonal* (a_3 negative, $\phi_o < 1/2$) symmetries. These have slightly different values of

Π_c and A_o/A, because of the symmetry breaking effect associated with $\bar{C}_o > 0$. Otherwise, this case appears similar to the one discussed by Leibler and Andelman [16] for $\bar{C}_o = 0$. If, on the other hand, $t < t_c$ (say, $t \sim \bar{C}_o$), we find, for *both* compositions ($\phi_o = 1/8$, $7/8$), only a single *hexagonal*, *large amplitude*, buckling state. The values of Π_c are still very close to one another, however, the values of A_o/A (or the wavelength to amplitude ratios) are now very different for the two compositions considered, differing by roughly a factor of two. (For example, using the lattice-gas estimates [28], $t = \bar{C}_o = 1/80$ Å^{-1}, and $\kappa = 30 k_B T$ we obtain $A_o/A = 0.1$ for $\phi_o = 1/8$, and $A_o/A = 0.056$ for $\phi_o = 7/8$.) This is because in one composition ($\phi_o < 1/2$) the cap energy is smaller than in the other composition ($\phi_o > 1/2$) if the selected buckling symmetry is hexagonal (rather than inverse hexagonal). Therefore, in the former case the monolayer can give up some of its cylindrical-like portion in favor of having more caps. This is similar to the situation in (bulk) worm-like micellar phases, in which the cap energy is used to control the micellar length [31].

Recall that our results for the transition are not sensitive to the equation of state $\Pi(A)$ in so far as the values Π_c and A_o/A are concerned. However, when more than one buckling state are competing, it is possible (in principle) that a transition to the second buckling state will follow (under further compression) the first (flat to buckled) transition. This possibility can be examined quantitatively only if the equation of state $\Pi(A)$ is known, and so will not be further discussed here.

Let us now consider the different possible isotherms. Around the buckling transition point the shape of the isotherm may take different forms depending on the coupling t. In Figure 4, we schematically depict the two equilibrium situations: (i) small amplitude buckling for $t > t_c$ (Fig. 4a), and (ii) large amplitude buckling for $0 < t < t_c$ (Fig. 4b). For the latter case, $0 < t < t_c$, we also depict a non-equilibrium situation (Fig. 4c), in which the equilibrium, large buckling, state is bypassed by the metastable, small buckling, state. This is quite a relevant scenario because, as discussed for the pure system case, the large energy barrier involved in the transition to the former state may hinder this equilibrium transition. We should emphasize that the precise value of Π_c depends on how far is the system from the point of phase separation within the flat monolayer. However, the general properties we discussed here are not sensitive to this value.

Some characteristics of the small buckling state ($t > t_c$) may be understood in a similar way to that discussed by Leibler and Andelman [16]. Putting $a_3 = a_4 = 0$ in equation (31), let us first minimize equation (32) in Fourier space over the field Ψ_q (the Fourier transform [32] of $\Psi(\mathbf{x})$). To *lowest order* in h, this leads to [33]

$$\Psi_{\mathbf{q}} \simeq \frac{\kappa t q^2}{a_2 + b q^2} h_{\mathbf{q}} \tag{37}$$

which, upon substitution in (32), leads to the effective free-energy for h (taken now only to quadratic order [33])

$$F_{\text{eff}}^{(h)} \simeq \frac{1}{2} \sum_{\mathbf{q}} \left(\sigma q^2 + \kappa q^4 - \frac{\kappa^2 t^2 q^4}{a_2 + b q^2} \right) h_{\mathbf{q}} h_{-\mathbf{q}} \tag{38}$$

It can be seen that the term in brackets is minimized by a different wavenumber q than the one chosen (by the higher order terms, omitted in Eq. (38)) for the "long fingers" state, $q_c \sim \bar{C}_o^{-1}$. Thus when the value of this coefficient at the preferred wavelength becomes sufficiently small (but still positive), *e.g.*, when t is large, a first order transition – induced by the higher order terms – can occur.

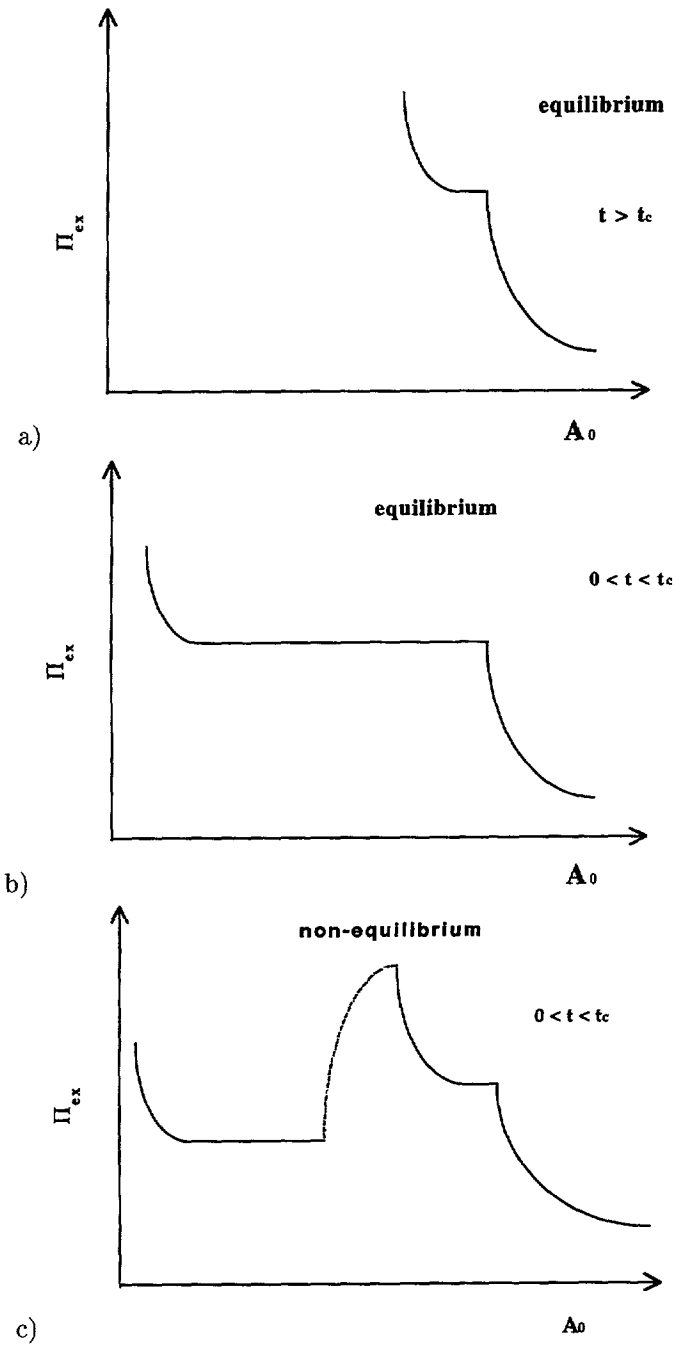

Fig. 4. — Schematic representation of possible pressure-area isotherms for different coupling constants t: (a) $t > t_c$, for which only small amplitude buckling is possible. (b) $0 < t < t_c$ (where t_c is the same one appearing in Fig. 3a), for which only large amplitude (long finger) hexagonal buckling appears. (c) Metastable isotherm for $0 < t < t_c$. The long finger, equilibrium, state is kinetically bypassed by a metastable, small amplitude, state. The metastable state can evolve by nucleation to the long finger state as the pressure is further increased and the nucleation barrier is lowered.

The situation is further simplified if the gradient terms in F_Ψ can be neglected, *i.e.*, if $bq_c^2 \ll a_2$. In this case we get, upon minimization over Ψ, $\Psi = (\kappa t/a_2)H$, leading to an effective bending energy

$$F_{\rm eff}^{(\kappa)} = F_\kappa - \frac{1}{2}\tilde{\kappa}\int_{A_o} {\rm d}^2x\sqrt{g}H^2 \tag{39}$$

where $\tilde{\kappa} = (\kappa t)^2/a_2$. When $\tilde{\kappa} \gg \kappa$ (large t), we may neglect F_κ in equation (39) and the effective bending energy is always negative for non-vanishing $\langle H^2\rangle$. The latter is stabilized by the surface tension term F_σ, leading to buckling with wavenumber $q_c^2 \simeq \sigma/\tilde{\kappa} \simeq \sigma a_2/(\kappa t)^2$ (in the small amplitude regime).

We conclude that the "small buckling" states (appearing for $t > t_c$), either the stripe for nearly symmetric compositions or the hexagonal for non-symmetric compositions, are induced purely by the composition-curvature coupling, as in the study of Leibler and Andelman [16]. In the "long fingers" (large buckling) state ($t < t_c$), on the other hand, the shape is determined mainly by the average spontaneous curvature $\bar{C}_o$, and the local composition is "slaved" to this preferred shape. (This latter case is somewhat similar to the study of Seifert [34] of curvature induced segregation in two-component vesicles.) Our theory thus appears sufficiently general to show a crossover between these two behaviours when the coupling strength t is varied relative to the average spontaneous curvature $\bar{C}_o$. The latter can be easily achieved by varying simultaneously the two spontaneous curvatures $C_o^{(1)}$ and $C_o^{(2)}$

4. Tilt-Curvature Coupling

A *single component* monolayer, sitting at the liquid-air interface, can also have inplane degrees of freedom which may couple to the local curvature, similar to the two-component case discussed in the previous section. An important degree of freedom for a monolayer in its liquid condensed phase is the molecular tilt with respect to the surface normal [1,35,36]. (For oil-water interfaces tilt is unlikely to occur because the oil molecules can fill up the space in-between the chains and thus minimize the van-der-Waals energy.) In fact, the tilt curvature coupling may be thought of as a mechanism for spontaneous curvature for chains which are not flexible enough to minimize their van-der-Waals energy by folding randomly in space [21,37]. Recently, the tilt-curvature coupling was used to explain the appearance of the ripple phase ($P_{\beta'}$) of phospholipid bilayers [21]. Here we shall use a similar approach for Langmuir monolayers. This involves two differences. First, unlike for bilayers in solutions, we may not assume that the surface tension is zero. Second, non-symmetric terms, which vanish for a bilayer on the basis of symmetry, must be taken into account when dealing with a monolayer.

We shall use the projection $\mathbf{m}$ of the tilt vector onto the local tangent surface as the order parameter. If we denote the surface normal as $\hat{\mathbf{N}}$, the unit vector along the chain axis as $\hat{\mathbf{n}}$, then the in-plane order parameter is $\mathbf{m} = \hat{\mathbf{n}} - (\hat{\mathbf{N}}\cdot\hat{\mathbf{n}})\hat{\mathbf{N}}$ (see Fig. 5). Similar to 3D liquid crystals [38], the free-energy density for $\mathbf{m}$ is assumed to have the following Landau-Ginzburg type expansion [21,35]

$$f_m = \frac{1}{2}C_1(\nabla\cdot\mathbf{m})^2 + \frac{1}{2}C_2(\nabla\times\mathbf{m})^2 + \frac{1}{2}D(\nabla^2\mathbf{m})^2 + \frac{1}{2}\delta|\mathbf{m}|^2 + \mu|\mathbf{m}|^4 - \lambda_s|\mathbf{m}|^2(\nabla\cdot\mathbf{m})\ . \tag{40}$$

Here, the $(\nabla\cdot\mathbf{m})^2$ and $(\nabla\times\mathbf{m})^2$ terms reflect the energy cost for in-plane splay and bend deformations of the tilt, respectively. The $(\nabla^2\mathbf{m})^2$ term is required for stability ($D > 0$) in case C_1 or C_2 are negative. The $|\mathbf{m}|^2$ and $|\mathbf{m}|^4$ terms compose the usual Landau free-energy which can describe a transition from zero ($\delta > 0$) to non-zero ($\delta < 0$) average tilt, but for simplicity we shall take $\delta > 0$ only, *i.e.*, the average tilt vanishes. (Nevertheless, the quartic

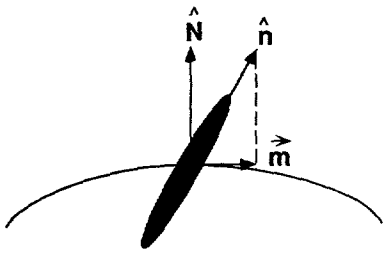

Fig. 5. — Surface normal unit vector $\hat{\mathbf{N}}$, tilt unit vector $\hat{\mathbf{n}}$, and tilt projection vector $\mathbf{m}$.

term with $\mu > 0$ is required for the stability of modulated structures, as shown below.) The last term, $|\mathbf{m}|^2(\nabla\cdot\mathbf{m})$, favors a splay deformation of $\mathbf{m}$ and is allowed here because of the *head-tail asymmetry* [35,39]. This differs from the bilayer case studied by Mackintosh *et al.* [21], for which $\lambda_s = 0$ due to the bilayer symmetry. In the latter case f_m has a simple Lifshitz free-energy form which is known to describe equilibrium modulated phases if either C_1 or C_2 are negative. As shown below, the presence of this cubic order term for a monolayer allows for the buckling transition to be first order.

The total free-energy density of the system includes surface tension, bending energy, the above tilt free-energy, and a coupling between the curvature and the tilt. The bending energy will be described according to equation (7) but with $C_o = 0$, since an effective spontaneous curvature already emerges in this model as a result of the tilt curvature coupling. Hence it will be sufficient to use this free-energy only to quadratic order in h. We shall also take the lowest possible order for the coupling [21,40]

$$f_c = \Lambda(\nabla^2 h)(\nabla\cdot\mathbf{m}) \,. \tag{41}$$

The total Gibbs free-energy of the monolayer, which includes the area constraint (2) and is analogous to equation (5), is

$$G_\sigma = [\gamma_o + f_o(\phi) - \sigma]\, A - (\gamma_o - \Pi_{ex})\, A_o + F_{hm} \tag{42}$$

with

$$F_{hm} = \sigma \int_{A_o} \mathrm{d}^2x\sqrt{g} + F_\kappa + F_m + F_c \tag{43}$$

and where $F_m = \int \mathrm{d}^2x\sqrt{g}f_m$ and $F_c = \int \mathrm{d}^2x\sqrt{g}f_c$.

We may now follow the same approach as in Section 2, but in addition to minimizations over A, A_o, and $\{h(\mathbf{x})\}$ we now have to minimize also over $\{\mathbf{m}(\mathbf{x})\}$. Minimizing over A and A_o we find again that at the buckling transition the surface tension coefficient is simply $\sigma = \gamma_o - \Pi_{ex}$. Because the free-energy F_{hm} is now taken only to quadratic order in h, we can first minimize exactly over h (or, equivalently, integrate out h), to give the linear relation in Fourier space

$$h_\mathbf{q} = \frac{i\Lambda\mathbf{q}\cdot\mathbf{m}_\mathbf{q}}{\sigma + \kappa q^2} \,, \tag{44}$$

where $h_\mathbf{q}$ and $\mathbf{m}_\mathbf{q}$ are the Fourier transforms [32] of $h(\mathbf{x})$ and $\mathbf{m}(\mathbf{x})$, respectively. Thus any modulation in $\mathbf{m}(\mathbf{x})$ necessarily leads to a modulation in $h(\mathbf{x})$, with just the same periodicity. Inserting equation (44) into F_{hm} yields an effective free-energy for $\mathbf{m}$

$$F_{\mathrm{eff}}^{(m)} = F_m - \frac{1}{2}\sum_\mathbf{q} \frac{\Lambda^2 q^2 (\mathbf{q}\cdot\mathbf{m}_\mathbf{q})(\mathbf{q}\cdot\mathbf{m}_{-\mathbf{q}})}{\sigma + \kappa q^2} \tag{45}$$

It can be seen that the coupling reduces the effective coefficient of the m^2 term and so helps to destabilize the unmodulated (flat) state. If $\lambda_s = 0$, a disorder to modulated (buckling) transition of second order type may occur at sufficiently large Λ. When $\lambda_s \neq 0$, which is possible for a monolayer, the transition will be first order.

Consider now the two following limiting cases: (i) When surface tension dominates over bending energy at the relevant wavelengths $q \sim q_c$, *i.e.*, if $\sigma \gg \kappa q_c^2$, the effective free-energy density in real space simply becomes

$$F_{\text{eff}}^{(m)} = \int \mathrm{d}^2x \left(f_m - \frac{\Lambda^2}{2\sigma} (\nabla(\nabla \cdot \mathbf{m}))^2 \right) \tag{46}$$

It is thus clear that large Λ^2/σ can induce a buckling (ordering) transition, which is either first ($\lambda_s \neq 0$) or second ($\lambda_s = 0$) order. Otherwise, for small Λ^2/σ and small D the phase diagram should be identical to that discussed by Mukamel *et al.* [39]. (ii) For small surface tensions $\sigma \ll \kappa q_c^2$, equation (46) has the same form as F_m with $C_1' = C_1 - (\Lambda^2/\kappa)$ replacing C_1. For $\lambda_s = 0$ it is identical to the one used in reference [21] for achiral lipid bilayers. For positive C_1' and non zero λ_s this effective free-energy is identical to the one used in references [35, 39] to describe modulated tilt structures in flat monolayers.

We now wish to calculate the critical pressure Π_c for the first order buckling transition. We use again a variation approach in which both $h(\mathbf{x})$ and $\mathbf{m}(\mathbf{x})$ have hexagonal symmetry taken to the first harmonic. (In the single harmonic approximation, the stripe and 2D square lattice buckling symmetries will have higher Π_{ex} than the 2D hexagonal symmetry, because the gradient-cubic term $|\mathbf{m}|^2(\nabla \cdot \mathbf{m})$ vanishes for the former shapes.) h thus obeys equation (19), and $\mathbf{m}$ is chosen, according to equation (44), to obey the vorticity condition $\nabla \cdot \mathbf{m} \sim \nabla^2 h$ (or $\mathbf{m} \sim \nabla h$), leading to

$$m_x = m_o \left[\sin(qx) - \frac{1}{2} \sin\left(q \frac{-x + \sqrt{3}y}{2} \right) + \frac{1}{2} \sin\left(q \frac{x + \sqrt{3}y}{2} \right) \right] , \tag{47}$$

$$m_y = \frac{\sqrt{3}}{2} m_o \left[\sin\left(q \frac{-x + \sqrt{3}y}{2} \right) + \sin\left(q \frac{x + \sqrt{3}y}{2} \right) \right] \tag{48}$$

This tilt modulation is depicted in Figure 6. We can see that $\mathbf{m}$ has a vortex when h is a local maximum and antivortex when h is a minimum. Substituting these expressions in equation (43) and minimizing over h_o, leads to (similar to Eq. (44))

$$h_o = \frac{\Lambda m_o q}{\sigma + \kappa q^2} \tag{49}$$

and to the effective free-energy density

$$f_{\text{eff}}^{(m)} = \frac{3}{4} \left(\delta + C_1 q^2 + D q^4 - \frac{\Lambda^2 q^4}{(\sigma + \kappa q^2)} \right) m_0^2 - \frac{3}{4} \lambda_s q m_0^3 + \frac{27}{8} \mu m_0^4 . \tag{50}$$

This free-energy density permits a first order transition to $m_o \neq 0$. We now have to minimize $f_{\text{eff}}^{(m)}$ over m_o and q. This is done in two stages. First, we minimize over m_o and solve $f_{\text{eff}}^{(m)} = 0$ (using $\sigma = \gamma_o - \Pi_{ex}$) for the q-dependent critical pressure

$$\Pi_c(q) = \gamma_o + \kappa q^2 - \frac{\Lambda^2 q^4}{\delta + C_1 q^2 + D q^4 - \dfrac{\lambda_s^2}{18\mu} q^2} \tag{51}$$

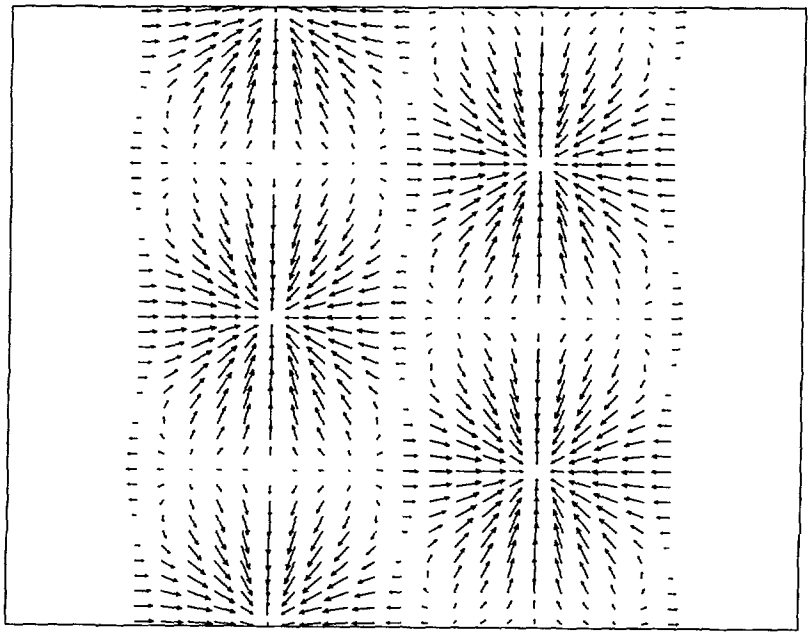

Fig. 6. — Vector order parameter **m** in the hexagonal buckling state. Note that a vortex of **m** corresponds to a maximum of h, and an antivortex to a minimum of h.

From this expression we obtain the condition that the minimal $\Pi_c(q)$ (varying q) be smaller than γ_o

$$C_1 + 2\sqrt{\delta D} < \frac{\Lambda^2}{\kappa} + \frac{\lambda_s^2}{18\mu} \tag{52}$$

To be more explicit we expand (51) for small q to obtain

$$\Pi_c(q) = \gamma_o + \kappa q^2 - cq^4 + dq^6 \tag{53}$$

(in which we assume $d > 0$) where

$$c = \frac{\Lambda^2}{\delta} \tag{54}$$

and

$$d = \frac{\Lambda^2}{\delta^2}\left(C_1 - \frac{\lambda_s^2}{18\mu}\right) \tag{55}$$

Upon minimization over q we obtain

$$q_c = \sqrt{\frac{c + \sqrt{c^2 - 3d\kappa}}{3d}} \tag{56}$$

and [41]

$$\Pi_c = \gamma_o - \frac{2c^3 - 9cd\kappa + 2(c^2 - 3d\kappa)^{3/2}}{27d^2} \tag{57}$$

The relative width of the plateau in the pressure area isotherm is obtained as

$$1 - \frac{A_o}{A} = \frac{4d\Lambda^2\lambda_s^2}{\sqrt{3}\mu^2(2c - \sqrt{c^2 - 3d\kappa})^2(c + \sqrt{c^2 - 3d\kappa})} \tag{58}$$

Note that for $\lambda_s = 0$ the plateau disappears and the transition becomes second order.

As mentioned earlier, the tilt-curvature coupling which we have considered here as a mechanism for buckling is similar to the mechanism suggested for the rippling transition of phospholipid bilayers [21]. We emphasize again the differences. Because of the inversion symmetry of bilayers, the gradient-cubic (λ_s) term in the free-energy is missing. So the transition from flat to rippled bilayer is of second order, instability, type, whereas for a monolayer it is always first order. Monolayers also endure surface tension, and so the pressure Π_{ex} is another controlling parameter for the transition. The bilayer ripple symmetry can be either 1D or 2D square lattice, whereas for a monolayer the 2D hexagonal symmetry is preferred. It could have been expected (contrary to our findings) that to buckle a Langmuir monolayer should be more difficult than to buckle a bilayer (in equilibrium) which is made of the same amphiphile, as the surface tension term contributes a positive energy for $\Pi_{ex} < \gamma_o$. However, because of the presence of the λ_s term, the transition is facilitated and becomes first order for non-zero λ_s.

Finally, because of the possible applicability to the experiment of reference [5], we would like to comment on the case of a *solid* (crystalline) monolayer with a nonzero tilt. In this situation we may expect that $|\mathbf{m}|$ (namely the tilt angle with respect to the surface normal) remains constant because of the large energy penalty which opposes deviations from the preferred value. However, *rotations* of $\mathbf{m}$ may be possible with a lower energy cost, and could be described by the free-energy (40). (This case is similar to the $P_{\beta'}^{(3)}$ of Chen *et al* [21].) Then, all terms involving $|\mathbf{m}|$ just contribute a constant; the λ_s term becomes linear in the tilt modulation and *vanishes* after integration. In order to satisfy $|\mathbf{m}| = m_o = \text{const.}$ we must choose [21] a *stripe* modulation (say, in the x-direction) in which $\mathbf{m}$ completes one rotation in a buckling period,

$$m_x = m_o\cos(qx), \quad m_y = m_o\sin(qx), \quad h = h_o\sin(qx)\ , \tag{59}$$

leading again to the relation (49) upon minimizing over h_o. The effective free-energy for $\mathbf{m}$ simply becomes

$$f_{\text{eff}}^{(m)} = \frac{1}{4}\left[(C_1 + C_2)q^2 + 2Dq^4 - \frac{\Lambda^2 q^4}{\sigma + \kappa q^2}\right] m_o^2\ . \tag{60}$$

A *second order* buckling transition to a stripe phase is obtained when the coefficient of m_o^2 first becomes negative. (Higher order gradient terms, such as $(\nabla \cdot \mathbf{m})^4$, can be added for stability.) Solving for the q-dependent critical pressure, and minimizing over q we find the wavenumber at the transition

$$q_c = \left(\frac{C_1 + C_2}{2D}\right)^{1/2} (\Theta - 1)^{1/2} \tag{61}$$

provided that $\Theta > 1$, where

$$\Theta = \frac{\Lambda}{\sqrt{(C_1 + C_2)\kappa}}\ . \tag{62}$$

The critical pressure is found to be

$$\Pi_c = \gamma_o - \frac{\Lambda}{D}\sqrt{(C_1 + C_2)\kappa}\left(\frac{\Theta}{2} + \frac{1}{2\Theta} - 1\right) \tag{63}$$

and is smaller than γ_o as expected. We note that for a solid monolayer κ is usually very large, $\kappa \sim 100 k_B T$. We may also expect that [42] $\Lambda \sim C_1 \sim \kappa$.

5. Discussion

5.1. OIL-WATER INTERFACES. — From the viewpoint of interfacial bending free-energy, we have found that spontaneous curvature permits the stability of very long fingers at positive interfacial tensions. However, since in our approach no overhangs were allowed (only single valued functions $h(\mathbf{x})$ were considered), it remains to explore the stability of these fingers against their own deformations. First, we note that when spontaneous curvature is *not* included, the usual Rayleigh instability in a cylindrical finger of radius $R \simeq C_o^{-1}$ cannot occur because the surface tension is smaller than the minimum required [43] $(3/2)\kappa/R^2$. However, when spontaneous curvature is included in the bending energy [44], linear analysis shows that a Rayleigh-like instability will occur provided that $RC_o > 1$ (using $\sigma = 1/2\kappa C_o^2$).

Moreover, the energy of small separate droplets can be lower than the energy of a cylindrical finger even if the Rayleigh-like instability does not occur. If, for example, we equate the volume of a long cylinder of radius $RC_o = 0.9$ to the total volume of spherical droplets of radius R_s, take $\sigma = 1/2\kappa C_o^2$ and neglect for simplicity the Gaussian rigidity $\bar{\kappa}$, we find that for $1.81 < R_s C_o < 2.26$ the interfacial energy of droplets is smaller than that of the cylinder. (This is true also for $R_s C_o > 163$.) The two states are therefore connected by an energy barrier and one needs a thermal fluctuation to initiate the transition. In addition, the free-energy of droplets in the bulk is further reduced by their entropy of mixing. We may thus conclude that the long finger profile can only be a metastable state. This conclusion is supported by roughness measurements of the interface between an oil phase and a droplet microemulsion phase in coexistence [45] (*i.e.*, in the regime of emulsification failure). The droplet radius can be used as a measure of C_o^{-1} In this case the surface tension is close to $1/2\kappa C_o^2$ but the interface roughness was found very small [45].

5.2. AIR-WATER SURFACES. — Considering pure Langmuir monolayers, the long finger solution is clearly hardly relevant. First, one needs to get very close to the spinodal point for it to be accessible by a thermal fluctuation; this occurs at high pressures, $\Pi_{ex} > \gamma_o$. Second, even if such a state is obtained, it is not likely to stay stable against multilayer formation. Hence, the monolayers which are expected to buckle are those involving tilt order parameter – which usually is the case in the liquid condensed phase – and those having more than one component, *e.g.*, the binary mixture discussed in Section 3.

Our predictions in the latter case involve only experimentally measurable quantities: the bending rigidity and the spontaneous curvature of each component. Thus the coupling strength t and the average spontaneous curvature $\tilde{C}_o$ (Sect. 3) can be found. Depending on the ratio of these two variables, the preferred buckling shape is either of small amplitude $qh_o \ll 1$ or of large amplitude $qh_o \gg 1$. The transition is first-order in both cases.

Most experiments, such as those done on lung surfactant [2] or fatty acid [10, 12, 13] monolayers, appear at present too limited to allow for a detailed comparison with the theory. It might be possible to interpret, in terms of our binary mixture theory, the experiment reported in reference [4] on a chlorosilane monolayer, in which a buckling state has been observed by grazing incidence X-ray scattering. The reported buckling amplitude is of order nm and the wavelength is about 10 μm, both in rough agreement with our "small amplitude buckling" results. The interpretation involves a few assumptions. First, we regard the partial polymerization (Si-O-Si backbone), which is believed to take place in this system, as reversible, *i.e.*, of equilibrium type. Second, we postulate that the polymerized domains have a different spontaneous curvature than those which are not polymerized. We note however that this "binary mixture" viewpoint is not entirely adequate for this system, and more direct observations are clearly needed.

6. Conclusions

In this paper we examined the stability of flat monolayers against their buckling. We considered both pure and mixed monolayers, in both cases the bending energy plays a major role. Our predictions suggest that, in the absence of molecular tilt with respect to the surface normal, a pure monolayer at the air-water surface will usually not buckle at positive tensions. In the presence of tilt, as in the case of many liquid condensed phases, the monolayer may more easily buckle *via* a mechanism similar to the rippling of a phospholipid bilayer. In mixtures, the monolayer can easily buckle to periodic structures due to a corresponding modulation in composition. The transition is almost always first-order due to the inherent up-down asymmetry of the monolayer, and so can be observed as a plateau in the isotherm.

A pure monolayer at the oil-water interface may buckle to a state of extremely long fingers. However, this state is likely to be metastable with respect to its breakage into droplets. It therefore remains to study the growth dynamics of these fingers which is competing with their breakage kinetics into droplets. Such a process has been previously suggested as a mechanism for spontaneous emulsification [6]. Since the radius of these quasi-cylindrical fingers is close to the spontaneous radius of curvature, so will be the radius of the droplets formed in such a process. The sign of the spontaneous curvature clearly determines if it is fingers (or droplets) of oil in water, or water in oil, which are formed, so that the microemulsion obtained in this way would be similar to its final equilibrium state. This is left for a future study.

Acknowledgments

We are grateful to David Andelman, Andrea Liu, Vladimir Kaganer, François Gallet, Bill Gelbart, David Mukamel, Michael Kozlov and Sam Safran for useful discussions, and to David Andelman for critical reading of the manuscript prior to its publication. This research was supported by the Israel Science Foundation administered by the Israel Academy of Sciences and Humanities, and by a research grant from the Edward D. and Anna Mitchell Endowment Fund for Excellence in Scientific Achievement. R.G. is an incumbent of the William T. Hogan and Winifred T. Hogan Career Development Chair.

References

[1] For reviews, see: Knobler C.M., *Adv. Chem. Phys.* **77** (1990) 397; Knobler C.M. and Deshai R., *Ann. Rev. Phys. Chem.* **43** (1992) 207; Möhwald H., *Ann. Rev. Phys. Chem.* **41** (1990) 441; McConnell H.M., *Ann. Rev. Phys. Chem.* **42** (1991) 171.

[2] Longo M.L., Bisagno A.M., Zasadzniski J.A.N., Bruni R. and Waring A.J., *Science* **261** (1993) 453.

[3] Milner S.T., Joanny J.-F. and Pincus P., *Europhys. Lett.* **9** (1989) 495.

[4] Bourdieu L., Daillant J., Chatenay D., Braslau A. and Colson D., *Phys. Rev. Lett.* **72** (1994) 1502.

[5] Saint-Jalmes A., Graner F., Gallet F. and Houchmandzadeh B., *Europhys. Lett.* **28** (1994) 565; Saint-Jalmes A., Graner F., Assenheimer M. and Gallet F., in "Short and long chains at interfaces", proceedings of the XXX rencontres de Moriond, J. Daillant, P. Guenoun, C. Marques, P. Muller and J. Tran Thanh Van Eds. (Editions Frontières, Gif-sur-Yvette, 1995) p. 229.

[6] Granek R., Ball R.C. and Cates M.E., *J. Phys. II France* **3** (1993) 829.
[7] Ries H.E. Jr, *Nature* **281** (1979) 287.
[8] Smith R.D. and Berg J.C., *J. Colloid Interface Sci.* **74** (1980) 273; De Keyser P. and Joos P., *J. Phys. Chem.* **88** (1984) 274.
[9] Pezron E., Cleason P.M., Berg J.M. and Vollhardt D., *J. Colloid Interface Sci.* **138** (1990) 245.
[10] McFate C., Ward D. and Olmsted J. III, *Langmuir* **9** (1993) 1036.
[11] Xue J., Jung C.S. and Kim M.W., *Phys. Rev. Lett.* **69** (1992) 474.
[12] Siegel S., Hönig D., Vollhardt D. and Möbius D., *J. Phys. Chem.* **96** (1992) 8157.
[13] Birdi K.S. and Vu D.T., *Langmuir* **10** (1994) 623.
[14] Friedenberg M.C., Fuller G.G., Frank C.W. and Robertson C.R., *Langmuir* **10** (1994) 1251.
[15] Weinbach S.P., Kjaer K., Grubel G., Legrand J.-F., Als-Nielsen J., Lahav M. and Leiserowitz L., *Science* **264** (1994) 1566.
[16] Leibler S. and Andelman D., *J. Phys. France* **48** (1987) 2013.
[17] Wang Z.G., *J. Chem. Phys.* **99** (1993) 4191.
[18] For a review, see: Seul M. and Andelman D., *Science* **267** (1995) 476.
[19] Robledo A., Varea C. and Talanquer V., *Phys. Rev. A* **43** (1991) 5736.
[20] Helfrich W., *Liq. Cryst.* **5** (1989) 1647.
[21] Chen C.-M., Lubensky T. and MacKintosh F.C., *Phys. Rev. E* **51** (1995) 504; Lubensky T.C. and MacKintosh F.C., *Phys. Rev. Lett.* **71** (1993) 1565.
[22] Taniguchi T., Kawasaki K., Andelman D. and Kawakatsu T., *J. Phys. II France* **4** (1994) 1333; Kawakatsu T., Andelman D., Kawasaki K. and Taniguchi T., *J. Phys. II France* **3** (1993) 971.
[23] For a review, see: Safran S.A., Pincus P.A. and Andelman D., *Science* **248** (1990) 354.
[24] Morantz D.J., *Colloids Surf. A: Phys. Eng. Asp* **92** (1994) 221.
[25] Kjaer K., Als-Nielsen J., Helm C.A., Laxhuber L.A. and Möhwald H., *Phys. Rev. Lett.* **58** (1987) 2224.
[26] Helfrich W.F., *Z. Naturforsch.* **28c** (1973) 693.
[27] The expansion to sixth order, combined with the single harmonic approximation, does give another local minimum at finite q with $q_c h_{oc} \simeq 0.5$, however, this minimum does not appear in the more accurate approach described here.
[28] In this approximation

$$\begin{aligned} s_o a_2 &= \frac{k_B T}{\phi_o(1-\phi_o)} - 4k_B T_c \\ s_o b &= k_B T_c + \kappa t^2/4 \\ s_o a_3 &= k_B T \left(\frac{1}{(1-\phi_o)^2} - \frac{1}{\phi_o^2} \right) \\ s_o a_4 &= 2k_B T \left(\frac{1}{(1-\phi_o)^3} + \frac{1}{\phi_o^3} \right) \end{aligned}$$

where s_o is the close packing area per molecule. For more details see references [29,30].
[29] Yokoi C.S.O., Coutinho-Filho M.D. and Salinas S.R., *Phys. Rev. B* **24** (1981) 4047.
[30] Granek R., Gelbart W.M., Bohbot Y. and Ben-Shaul A., *J. Chem. Phys.* **101** (1994) 4331.
[31] For a review, see: Cates M.E. and Candau S.J., *J. Phys. C (Cond. Matter)* **2** (1990) 6869.
[32] The 2D Fourier transform $u_{\mathbf{q}}$ of the function $u(\mathbf{x})$ is

$$u_{\mathbf{q}} = (1/A_o) \int_{A_o} \mathrm{d}^2 x \; u(\mathbf{x}) \exp(i\mathbf{q} \cdot \mathbf{x})$$

[33] In fact, this minimization can be done exactly because the free-energy is now assumed quadractic in Ψ. This will lead to "renormalization" of the higher order terms in $F_{\rm eff}^{(h)}$, omitted in equation (38).
[34] Seifert U., *Phys. Rev. Lett.* **70** (1993) 1335.
[35] Selinger J.V. and Selinger R.L.B., *Phys. Rev. E* **51** (1995) R860.
[36] Kaganer V.M., Osipov M.A. and Peterson I.R., *J. Chem. Phys.* **98** (1993) 3512.
[37] We thank V. Kaganer for suggesting this possibility.
[38] de Gennes P.-G., The Physics of Liquid Crystals (Oxford University, London, 1974).
[39] Jacobs A.E. and Mukamel D., *J. Stat. Phys* **58** (1990) 503; Jacobs A.E., Goldner G. and Mukamel D., *Phys. Rev. A* **45** (1992) 5783.
[40] This can be obtained using the more general coupling term $\Lambda\nabla\cdot\hat{\mathbf{N}}\nabla\cdot\hat{\mathbf{n}}$ where $\hat{\mathbf{N}}$ is the surface normal and $\hat{\mathbf{n}}$ is the unit vector along the chain axis.
[41] Note however that in this small q approximation, the condition for having $\Pi_{\rm c} < \gamma_0$ is changed to $C_1 < 3\Lambda^2/\kappa + \lambda_{\rm s}^2/(18\mu)$.
[42] This is because one source for the three free-energy terms involved, $(\nabla\cdot\mathbf{m})^2$, $(\nabla^2 h)^2$, and the coupling term $(\nabla^2 h)(\nabla\cdot\mathbf{m})$, can be a single free-energy term $(\nabla\cdot\hat{\mathbf{n}})^2$, where $\hat{\mathbf{n}}$ is the unit vector along the chain axis. By substituting $\hat{\mathbf{n}} = \mathbf{m} + \mathbf{N}\cos(\theta)$, where θ is the tilt angle, these three terms are obtained (with approximately the same coefficients in front, unless $\theta \simeq \pi/2$).
[43] Granek R. and Olami Z., *J. Phys. II France* **5** (1995) 1349; Bar-Ziv R. and Moses E., *Phys. Rev. Lett.* **73** (1994) 1392.
[44] Granek R. and Hu J.-G., to be published.
[45] Langevin D. and Meunier J., in Micelles, Membranes, Microemulsions and Monolayers, W. M. Gelbart, A. Ben-Shaul and D. Roux Eds. (Springer, N.Y., 1994).